Fuel Processing Technology 91 (2010) 169–174

Contents lists available at ScienceDirect

Fuel Processing Technology

journal homepage: www.elsevier.com/locate/fuproc

Ultradispersed particles in heavy oil: Part II, sorption of $H_2S_{(g)}$

Nashaat N. Nassar [a,*], Maen M. Husein [a,b,*], Pedro Pereira-Almao [a,b]

[a] Alberta Ingenuity Centre for In-Situ Energy, University of Calgary, Calgary, Alberta, Canada
[b] Department of Chemical and Petroleum Engineering, University of Calgary, Calgary, Alberta, Canada

ARTICLE INFO

Article history:
Received 3 January 2009
Received in revised form 5 August 2009
Accepted 17 September 2009

Keywords:
H_2S
Sorption
Heavy oil
Metal oxide
Sorbent

ABSTRACT

During steam assisted gravity drainage for heavy oil recovery aqua-thermolysis reactions take place, whereupon gaseous hydrogen sulfide, $H_2S_{(g)}$, is produced. A method to capture $H_2S_{(g)}$ and convert it into a chemically inactive species is deemed necessary for sustaining *in-situ* recovery and upgrading. Part I of the current study explored the formation and stabilization of colloidal FeOOH particles in heavy oil matrices. In this Part, we evaluate the $H_2S_{(g)}$ sorption ability of these particles as well as other metal oxide/hydroxide particles. Furthermore, the effect of mixing and temperature on $H_2S_{(g)}$ sorption was investigated. Results showed that the rate and capacity of $H_2S_{(g)}$ sorption increased as the concentration of FeOOH increased. Mixing, on the other hand, had insignificant effect on the sorption capacity, however it improved the sorption kinetics. In addition, *in-situ* prepared colloidal particles showed better reactivity towards $H_2S_{(g)}$ than commercial α-Fe_2O_3 nanoparticles. Temperature had an adverse effect on the $H_2S_{(g)}$ sorption capacity of FeOOH. This was attributed to a change in chemical structure of FeOOH as the temperature increased. Nevertheless, *in-situ* prepared ZnO colloidal particles completely removed $H_2S_{(g)}$ even at high temperatures.

Crown Copyright © 2009 Published by Elsevier B.V. All rights reserved.

1. Introduction

With the continuous depletion of the world's supply of conventional oil, there is an increasing demand for recovering and upgrading of heavy oil and bitumen to meet current and future energy needs of the world. However, due to the high viscosity and specific gravity of heavy oil its ability to flow within the reservoir is low [1–4]. Two thermal recovery techniques have been employed to raise the temperature of heavy oil and reduce its viscosity, *in-situ* combustion and steam injection. Steam injection, known as steam assisted gravity drainage (SAGD), is the most common and effective recovery method [5,6]. In SAGD, the steam is used as the heat carrier to increase the temperature and reduce the viscosity of heavy oil, and consequently reduce the flow resistance of heavy oil through porous media which increase the yield and production rate [5,6]. However, heavy oil recovering and upgrading has been proven to be environmentally unfriendly [7]. During viscosity reduction a number of chemical reactions between steam and heavy oil take place [2,8,9]. The production of hydrogen sulfide and carbon dioxide in addition to other minor gaseous pollutants is common during SAGD process [2,8,9]. Aqua-thermolysis, which describes the chemical interaction of high temperature and high pressure steam with reactive components of heavy oil, leads to breaking the C—S bond in heavy oil [2]. $H_2S_{(g)}$ is a highly toxic and odorous gas that can impact underground water and contribute for the acid rain formation as well. Moreover, $H_2S_{(g)}$ can cause pipeline corrosion, poison catalysts and limit plant lifetime [10]. Thus, a method to capture $H_2S_{(g)}$ and convert it to a chemically inactive product during *in-situ* recovery and upgrading is necessary.

In a previous work, we showed that ultradispersed colloidal FeOOH particles formed *in-situ* in 1-methyl naphthalene continuous oil phase by means of (w/o) microemulsion methods effectively converted $H_2S_{(g)}$ into FeS and S^0 [1]. In addition, our previous work showed that commercial α-Fe_2O_3 nanoparticles as well as soluble $FeCl_{3(aq)}$ dispersed in the same background microemulsions were ineffective towards $H_2S_{(g)}$ capturing within the residence time of the gas bubbles [1]. Part I of the current work investigated the formation and stabilization of colloidal FeOOH particles in heavy oil matrices. Results from Part I showed that appreciable concentration of colloidal FeOOH particles could be maintained stable for more than 48 h. Part II of the current investigation explores the effectiveness of the ultradispersed colloidal FeOOH particles in capturing $H_2S_{(g)}$ while it bubbles through the heavy oil. *In-situ* prepared FeOOH were compared with commercial iron oxide nanoparticles. In addition, other metal oxides; including MgO, CaO and ZnO were tested towards $H_2S_{(g)}$ sorption, especially at higher temperature. Packed columns of these metal oxide particles have been shown to effectively remove $H_2S_{(g)}$ [10–14]. The present work holds great promise for online removal of $H_2S_{(g)}$ during *in-situ* heavy oil recovery and upgrading [7]. Example of potential application of *in-situ* prepared colloidal metal oxide particles is illustrated in Fig. 1.

* Corresponding authors.
E-mail addresses: nassar@ucalgary.ca (N.N. Nassar), maen.husein@ucalgary.ca (M.M. Husein).

0378-3820/$ – see front matter. Crown Copyright © 2009 Published by Elsevier B.V. All rights reserved.
doi:10.1016/j.fuproc.2009.09.008

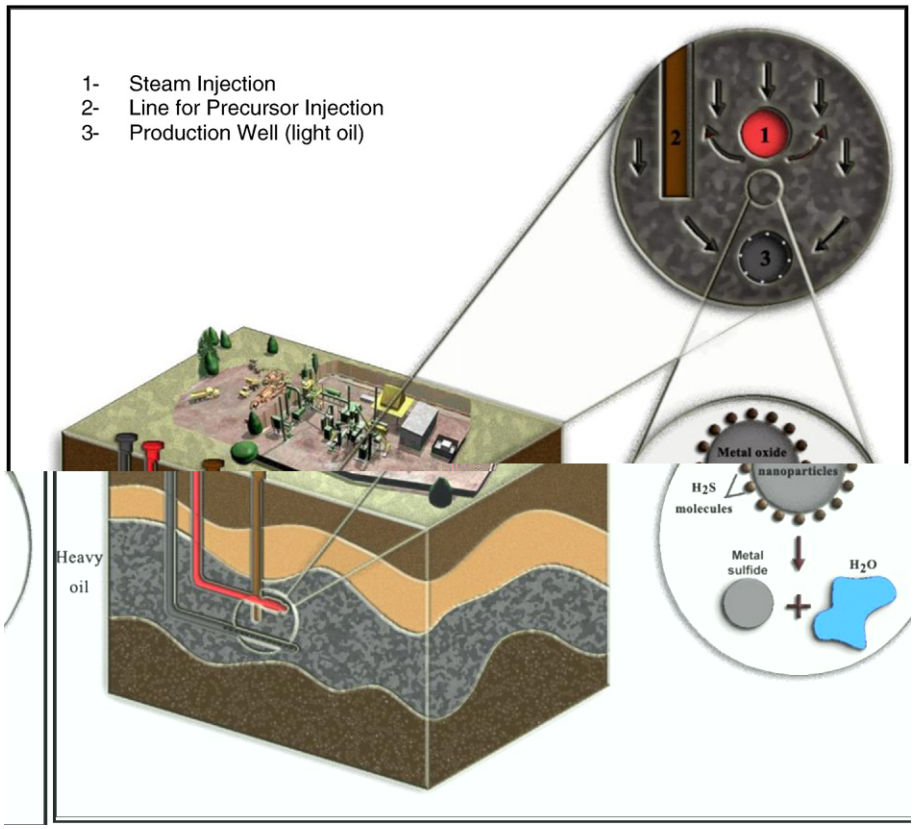

Fig. 1. Model for *in-situ* preparation of metal oxide sorbents during heavy oil recovering and upgrading.

2. Experimental

2.1. Materials

The heavy oil matrix was obtained by mixing vacuum gas oil, VGO, and vacuum residue, VR, belonging to bitumen from Athabasca, Alberta. The following metal precursors were used to prepare the corresponding colloidal metal oxide/hydroxide particles; including $FeCl_3$ (Laboratory grade, Fisher Scientific, Toronto, ON), $Ca(NO_3)_2.4H_2O$ (99%, Fisher Scientific, Toronto, ON), $MgCl_2.6H_2O$ (99%, Fisher Scientific, Toronto, ON) and $ZnCl_2$ (99.99%, Alfa Aesar, Toronto, ON). Sodium hydroxide (5.0N, Alfa Aesar, Toronto, ON) was used as the precipitating agent.

2.2. Preparation of the ultradispersed sorbent

Details on the *in-situ* preparation of the colloidal iron oxide/hydroxide particles in heavy oil matrices have been included in Part I of the current investigation. The preparation of the Mg, Ca and Zn oxides/hydroxides followed exactly the same procedure. The composition of the heavy oil matrix was maintained at 80 wt.% VGO, 20 wt.% VR and 2.5 vol.% of water or aqueous precursor solutions were used.

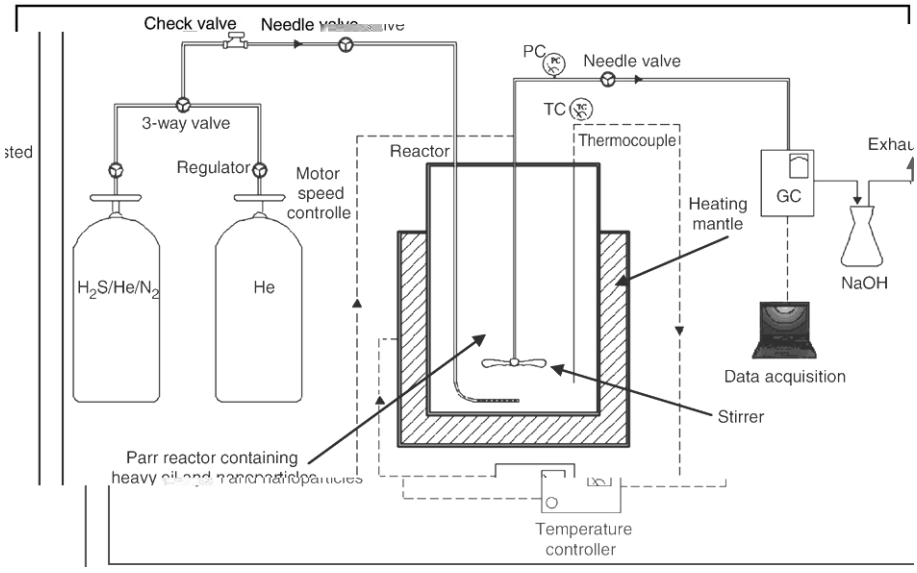

Fig. 2. Schematic diagram of the $H_2S_{(g)}$ sorption experiment.

The heavy oil containing colloidal metal oxide/hydroxide particles was poured into the reactor vessel of the experimental setup. To further investigate the ability of heavy oil matrices to disperse ex-situ prepared particles for the sorption of $H_2S_{(g)}$ by commercially available anhydrous crystalline iron (III) oxide nanoparticles, α-Fe_2O_3 (Nanostructured & Amorphous Materials, Inc., Houston, TX), was attempted. Particle diameter of α-Fe_2O_3 ranged from 20 to 50 nm, as per manufacturer. The α-Fe_2O_3 particles were dispersed in the heavy oil matrix by sonication for 30 min.

2.3. Experimental setup

The $H_2S_{(g)}$ sorption experiments were carried out in the setup shown in Fig. 2 [1]. A high pressure 100 ml reactor vessel (Parr Instrument Company, Moline, IL) equipped with a gauge pressure, a heating band with temperature controller, and stirrer with speed controller was used to bubble $H_2S_{(g)}$-containing feed streams through the heavy oil matrix. The reactor is capable of handling a pressure up to 2000 psi and a temperature up to 350 °C. The feed streams contained 200 ppm H_2S and 1000 ppm N_2 in He (balance). The flowrate of the gas stream was controlled at the outlet by a flow controller (5850S, Brooks Instruments, Fremont, CA). A three-way valve is fitted between the gas cylinder containing 200 ppm $H_2S_{(g)}$ and the one containing pure He, and a one-way check valve is placed in the gas line to avoid reverse flow. The exit stream of the reactor was allowed into a gas chromatograph, GC (SRI 8610C, SRI Instruments, Torrance, CA), having a FPD detector.

2.4. $H_2S_{(g)}$ sorption experimental procedure

A 50-ml sample of heavy oil with or without colloidal metal oxide/hydroxide particles was added to the reactor vessel. Then, stirring at 60 rpm commenced, unless otherwise noted. Leak test was performed by pressurizing the reactor with pure He up to 300 psi. A 1% change in pressure per hour was adopted as the maximum allowable pressure decrease during the leak test. A 200 psi pressure was maintained after the termination of the leak test. $He_{(g)}$ was used for purging the system until $O_{2(g)}$ disappeared completely, as measured by the GC. Following purging, the reactor was heated up to the desired temperature. When the reactor working pressure and temperature were attained, the actual sorption experiments start by switching of the inlet gas from pure $He_{(g)}$ to $H_2S_{(g)}$-containing feed. At this point the zero reaction time for the sorption experiment was considered. The reaction was carried out until no significant change in $H_2S_{(g)}$ inlet and outlet concentration was appeared. The reactor was cooled down to room temperature and purged with pure $He_{(g)}$ at the end of the run. The heavy oil sample was discharged from the reactor vessel, and the reactor vessel and assembly were washed with toluene. The heavy oil-toluene products were recovered for further analysis by using an evaporator. Due to artifacts stemming from heavy oil components, X-ray provided inconclusive patterns of the particles collected before or after $H_2S_{(g)}$ sorption. These artifacts could not be removed by washing the particles, after high speed centrifugation, with different solvents, including toluene. Burning the sample to remove heavy oil composition was not considered, since burning impacts particle composition. The results of $H_2S_{(g)}$ sorption were plotted as the fraction of the $H_2S_{(g)}$ concentration in the effluent gas from the reactor vessel, $C_{H_2S(g),e}$, over that in the feed stream, $C_{H_2S(g),i}$, according to Eq. (1).

$$f = \frac{C_{H_2S_{(g)},e}}{C_{H_2S_{(g)},i}} \quad (1)$$

3. Results and discussion

Even though particle characterization could not be performed, X-ray diffraction patterns of FeOOH nanoparticles prepared using the same procedure, precursors and under the same conditions, but in (w/o) microemulsions confirmed the formation of FeOOH nanoparticles [15]. It was, hence, concluded that FeOOH particles were obtained in this study. X-ray diffraction pattern of the spent particles, after $H_2S_{(g)}$ sorption, showed the formation of $FeS_{(s)}$ and $S^0_{(s)}$, as per our previous study [1], which is characteristic of reductive solubilization of FeOOH [16–18].

3.1. Sorption mechanism

It is suggested that the sorption of $H_2S_{(g)}$ is a two stage process [1,10], in the first stage adsorption of $H_2S_{(g)}$ takes place whereby $H_2S_{(g)}$ diffuses through the heavy oil emulsions/microemulsions until it reaches the surface of the colloidal metal oxide/hydroxide particle where $H_2S_{(g)}$ is adsorbed onto the surface. In the second stage sorption takes, whereby $H_2S_{(g)}$ at the solid surface reacts readily with the bulk of metal oxide/hydroxide to form metal sulfide, elemental sulfur and water following Reaction (2) for FeOOH colloidal particles [16–18]. The dominant of the stages depends heavily on the surface area/g of the colloidal particles. The reaction ceases either when all solid oxide is reacted or when the formed sulfide shell acts as a mass transfer barrier that limits the diffusion process. This retardation is much more pronounced for larger particles.

$$3H_2S + 2FeOOH \rightarrow 2FeS_{(s)} + S^0_{(s)} + 4H_2O \quad (2)$$

3.2. Effect of colloidal FeOOH concentration

Fig. 3 shows the fraction of $H_2S_{(g)}$ concentration in the effluent gas from the reactor over that in the feed, *f*, as a function of time for 0, 2.5 and 6.2 mM concentration of colloidal FeOOH particles. The experimental conditions were 25 °C, 200 psi, 40 cm^3/s, and 60 rpm mixing.

A comparison between the different curves in Fig. 3 shows that $H_2S_{(g)}$ is effectively removed with the aid of colloidal FeOOH particles. Higher concentration of colloidal FeOOH particles increased the sorption capacity of the system. Calculation of moles of $H_2S_{(g)}$ reacted until the break point indicates that a stoichiometric amount of $H_2S_{(g)}$ was readily reacted as per Reaction (2). This suggests that neither mass transfer nor reaction kinetics limited the interaction between $H_2S_{(g)}$ and the colloidal FeOOH particles within the residence time of the gas. This, in turn, indicates that dispersion by the heavy oil matrices and mixing was sufficient to grant enough contact between

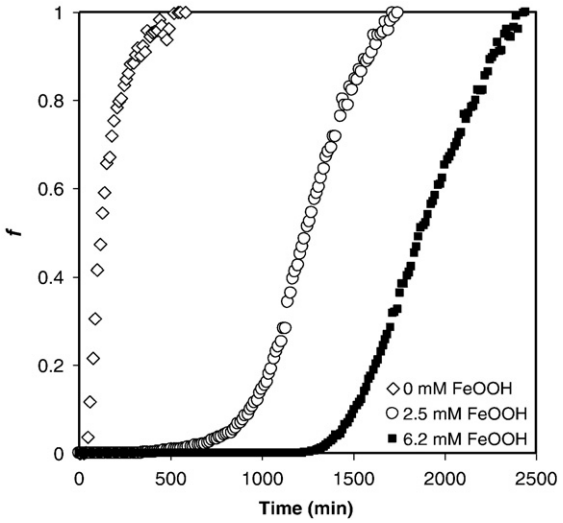

Fig. 3. $H_2S_{(g)}$ breakthrough curves presented as *f* versus time in the presence and absence of colloidal FeOOH particles in heavy oil matrix. Experimental conditions: 25 °C, 200 psi, 40 cm^3/min feed flow and 60 rpm mixing.

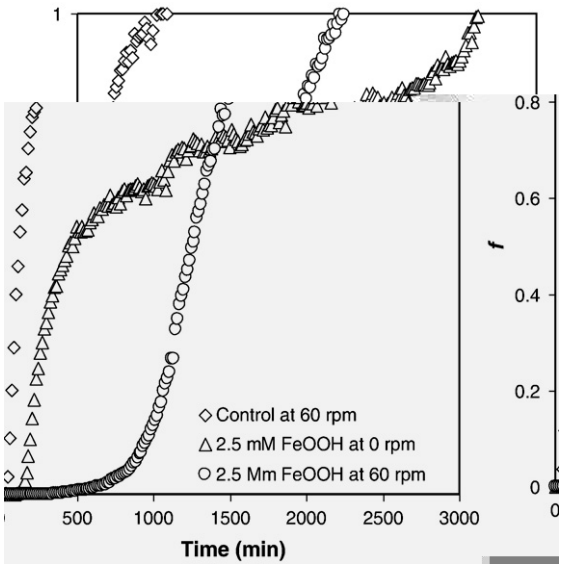

Fig. 4. $H_2S_{(g)}$ breakthrough curves presented as *f* versus time at 0 and 60 rpm mixing. Control sample contains no colloidal FeOOH particles. Experimental conditions: 25 °C, 200 psi and 40 cm^3/min.

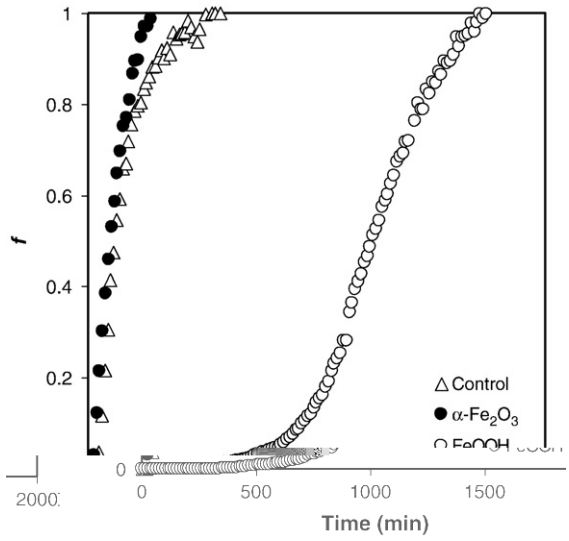

Fig. 5. *f* versus time for commercial α-Fe_2O_3 nanoparticles dispersed in heavy oil matrix. *f* for the control sample and the *in-situ* prepared colloidal FeOOH particles are provided for comparison. Experimental conditions: 25 °C, 200 psi, 40 cm^3/min feed flow and 60 rpm mixing.

the $H_2S_{(g)}$ and the colloidal particles. Similar observations were reported in our previous study with CTAB/butanol/water/1-methyl naphthalene microemulsion containing FeOOH nanoparticles [1].

3.3. Effect of mixing

In order to evaluate the dispersion of the colloidal particles granted by heavy oil matrix alone, runs without mixing were performed. It is important to know that limited mixing can be provided within reservoir environment during heavy oil recovery and upgrading. Therefore, the success of the *in-situ* sorption of the $H_2S_{(g)}$ hinges upon the dispersion granted by the heavy oil matrix.

Fig. 4 compares the $H_2S_{(g)}$ breakthrough curves of the 2.5 mM colloidal FeOOH particles with and without mixing at 25 °C, 200 psi, and 40 cm^3/min. Control run containing no colloidal FeOOH particles with mixing was provided for comparison. As can be seen, the sample with mixing showed the longest onset time compared with the one without mixing. Furthermore, with mixing, the breakthrough curve was sharp as most of the colloidal FeOOH particles were utilized at the onset point as per Reaction (2). On the other hand, without mixing, the breakthrough curve is further extended and less than one-quarter of the colloidal FeOOH is utilized at the onset point. Interestingly, the area above the curves for the two runs differed only by 20%. The difference in the areas above the breakthrough curves of the control run and the other samples is proportional to the amount of $H_2S_{(g)}$ sorbed by colloidal FeOOH particles. This suggests that in both scenarios, mixing and without mixing, $H_2S_{(g)}$ was mostly sorbed. However, kinetics of $H_2S_{(g)}$ sorption is higher with mixing.

3.4. Commercial α-Fe_2O_3 as sorbents

α-Fe_2O_3 has been reported as a good sorbent of $H_2S_{(g)}$ [10,19]. In our previous investigation [1], we reported almost zero sorption capacity of α-Fe_2O_3. This finding was attributed to a poor dispersion of α-Fe_2O_3 particles conferred by CTAB/butanol/water/1-methyl naphthalene microemulsions. Since the current investigation is involving a different system, this experiment will shed some lights on the dispersion capability of the heavy oil matrix towards ex-situ prepared particles.

Fig. 5 shows $H_2S_{(g)}$ breakthrough curves for a control sample, a sample containing α-Fe_2O_3 nanoparticles and a sample containing 2.5 mM *in-situ* prepared colloidal FeOOH particles obtained at 25 °C, 200 psi, 40 cm^3/min and 60 rpm. In order to maintain the same molar concentration of iron in both cases, the concentration of commercial α-Fe_2O_3 nanoparticles was set at 1.25 mM, which was half the corresponding concentration of the *in-situ* prepared particles.

As can be seen, the sorption of $H_2S_{(g)}$ by the commercial α-Fe_2O_3 nanoparticles was insignificant. This observation was also supported by the color of the precipitated particles formed at the bottom of the reactor vessel at the end of the experiment. The commercial nanoparticles remain red-brown, which indicates minimum conversion to iron sulfide is formed; while the *in-situ* prepared particles turned into black due to the formation of iron sulfide. One explanation of these results is that the heavy oil matrix does not provide enough dispersion for the α-Fe_2O_3 particles, which created a mass transfer barrier. This supports the fact that *in-situ* prepared particles provide better sorption capacity compare with the ex-situ prepared ones. Another explanation relate to the

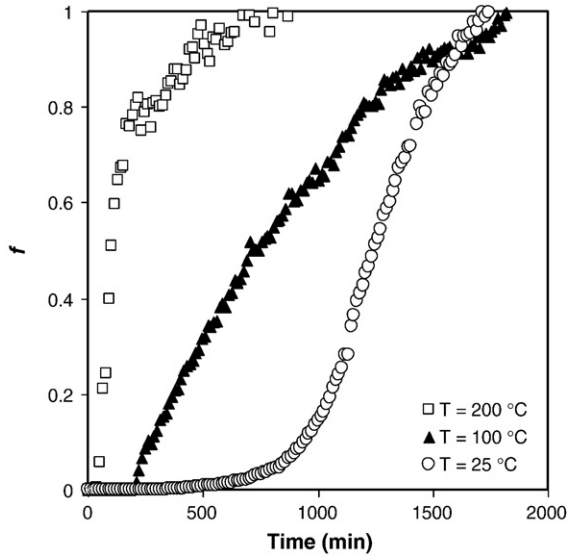

Fig. 6. *f* versus time for heavy oil matrices containing 2.5 mM *in-situ* prepared FeOOH particles at different temperatures. Experimental conditions: 200 psi, 40 cm^3/min feed flow and 60 rpm mixing.

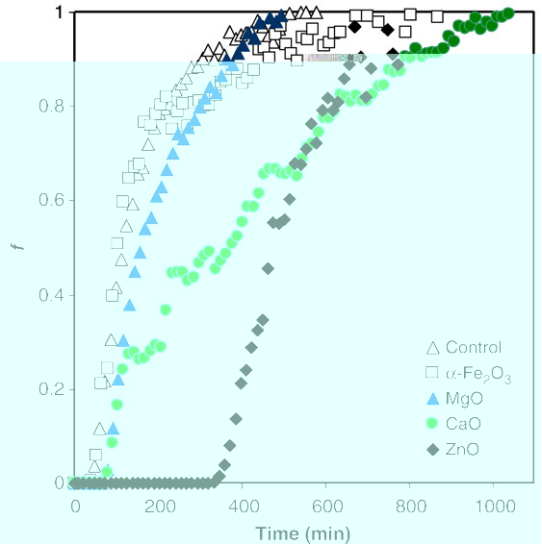

Fig. 7. *f* versus time for 2.5 mM different types of *in-situ* prepared metal oxide colloidal particles in heavy oil matrix. Experimental conditions: 200 °C, 200 psi, 40 cm^3/min feed flow and 60 rpm mixing.

chemical structure of iron oxide. It has been reported that amorphous iron hydroxide react readily and more extensively with H_2S than iron oxide with organized crystal structure, such as hematite [16,18–20]. Therefore, within the residence time of the $H_2S_{(g)}$ sorption by α-Fe_2O_3 nanoparticles was too slow.

3.5. Effect of temperature

As heavy oil recovery and upgrading take place at high temperatures, it was necessary to study the effect of temperature on the stability and reactivity of the *in-situ* prepared colloidal FeOOH particles. Most of the reported literature studied the ex-situ removal of $H_2S_{(g)}$ at high temperatures (>350 °C) [10,21] and little work focused on the removal of $H_2S_{(g)}$ at temperature less than 200 °C [10,14]. It is believed that, low temperature $H_2S_{(g)}$ absorption improves the energy efficiency and reduces the environmental impact [12]. In this experiment, the heavy oil temperature was increased from 25 to 200 °C at 200 psi, 40 cm^3/min and 60 rpm of mixing. The results are given at various temperatures in Fig. 6.

Fig. 6 shows that the breakthrough curves differed in their onset time and shape as the temperature increased. The onset time of $H_2S_{(g)}$ shifted to the left, indicating lower rate of sorption and lower sorption capacity at higher temperatures. It is worth noting that FeOOH can transform to α-Fe_2O_3 and β-FeOOH as well as α-FeOOH as the temperature increases [22]. α-Fe_2O_3 is the most thermodynamically stable phases at temperatures above 100 °C [23]. Calculations using the thermodynamic equilibrium software FactSage® performed to determine the affinity of α-Fe_2O_3 towards the $H_2S_{(g)}$ at 200 °C showed that the reaction of α-Fe_2O_3 with $H_2S_{(g)}$ is thermodynamically unfeasible. This, we believe, explains the early evolution of $H_2S_{(g)}$ in Fig. 6 at 200 °C. The color of the precipitated particles formed at the bottom of the reactor at the end of the experiment was red-brown, which is the color of α-Fe_2O_3.

3.6. Other metal oxide sorbents

Since FeOOH failed to remove $H_2S_{(g)}$ at high temperature; Ca, Mg and Zn oxide/hydroxide colloidal particles were prepared following the same procedure and tested towards the $H_2S_{(g)}$ removal. The temperature was fixed at 200 °C and mixing commenced at 60 rpm. At this temperature, the hydroxide form of this metal would convert to the oxide. The concentration of the different metal oxides was 2.5 mM.

Fig. 7 shows that the $H_2S_{(g)}$ breakthrough curves in the presence of the different colloidal metal oxide particles. The curves for the control sample and the heavy oil matrix containing 2.5 mM FeOOH was provided for comparison. It is evident from Fig. 7 that the rate of sorption is strongly dependent on the metal oxide. The onset time of $H_2S_{(g)}$ followed the sequence ZnO > CaO > MgO > Fe_2O_3. Table 1 presents the amount of metal oxide consumed at the onset time and compares that with the stoichiometric amount calculated as per the general Reaction (3), where M stands for any of the metal, except Fe_2O_3 which should follow Reaction (4) [19].

$$MO_{(s)} + H_2S_{(g)} \rightarrow MS_{(s)} + H_2O_{(g)} \quad (3)$$

$$Fe_2O_{3(s)} + 3H_2S_{(g)} \rightarrow Fe_2S_{3(s)} + 3H_2O_{(g)} \quad (4)$$

As can be seen in Table 1, ZnO was completely consumed at the onset time suggesting its sorption kinetics was faster than the residence time of $H_2S_{(g)}$ in the reactor vessel.

4. Conclusions

The $H_2S_{(g)}$ sorption ability of the *in-situ* prepared metal oxide/hydroxide colloidal particles in heavy oil matrix was demonstrated. *In-situ* prepared colloidal FeOOH particles were more effective in $H_2S_{(g)}$ removal than ex-situ prepared α-Fe_2O_3 nanoparticles dispersed in the heavy oil matrix. This, however, might be attributed to a different crystal structure of the two particles. The sorption capacity of the colloidal FeOOH particles is inversely proportional to temperature. This was attributed to structural change in the iron oxide/hydroxide as temperature increased. Mixing the heavy oil matrix had insignificant effect on the sorption capacity of the colloidal particles, while improved the sorption kinetics of the colloidal particles. The *in-situ* prepared zinc oxide particles were more efficient for the removal of $H_2S_{(g)}$ at 200 °C than the other metal oxides considered in this study.

Acknowledgements

We acknowledge the financial support from the Alberta Ingenuity Centre for In-Situ Energy, University of Calgary. Thanks to Mr. Luis Patruyo for helping in the experimental setup and to Mrs. Maha AbuHafeetha for drawing the model and the experimental diagrams.

Table 1
Mole of the different metal oxides consumed at the onset time as calculated theoretically from Reactions (2), (3) and (4) at 2.5 mM and 200 °C.

Type of oxide	Temp. °C	Conc. mM	Onset time (min)	Available (mmol)	Consumed at the onset time (mmol)	Unconsumed (mmol)
Control	25	0	45	–	–	–
Fe_2O_3	200	2.5	45	0.12	0.00	0.12
MgO	200	2.5	78	0.127	0.011	0.116
CaO	200	2.5	78	0.127	0.011	0.116
ZnO	200	2.5	371	0.125	0.11	0.015

References

[1] M.M. Husein, L. Patruyo, P. Pereira-Almao, N.N. Nassar, Scavenging H2S(g) from oil phases by means of ultradispersed sorbents, J. Colloid Interface Sci. (submitted for publication).

[2] J.B. Hyne, J. W. Greidanus, J. D. Tyrer, D. Verona, P.D. Clark, R.A. Clarke and J.H.F. Koo, Aqua-thermolysis of heavy oils. Proceedings, 2nd International Conference on Heavy Crude and Tar Sands. Caracas, Venezuela, 1982, Chapter 9, Vol. I.

[3] A.S.M. Farouq, Oil Recovery by Steam Injection, Producers Publishing Co. Inc., Bradford, PA, 1970.

[4] B.T. Willman, V.V. Valleroy, G.W. Runberg, A.J. Cornelius, L.W. Powers, Laboratory studies of oil recovery by steam injection, J. Petrol. Technol. 13 (1991) 681–690.

[5] R.M. Butler, Thermal Recovery of Oil and Bitumen, Prentice-Hall, Englewood, 1991 pp. 285–359.

[6] S.S. Saskoil, R.M. Butler, The production of conventional heavy oil reservoirs with bottom water using steam-assisted gravity drainage, J. Can. Pet. Technol. 29 (1990) 78–86.

[7] AICISE 2008. The Alberta Ingenuity Centre for *In Situ* Energy: AICISE Fact Sheet [Online]. Available: http://www.aicise.ca/ [17 April 2008].

[8] P.D. Clark, J.B. Hyne, Studies on the chemical reactions of heavy oils under steam stimulation, AOSTRA J. Res. 6 (1990) 29–39.

[9] P.D. Clark, J.B. Hyne, Steam-oil chemical reactions: mechanisms for the aquathermolysis of heavy oils, AOSTRA Journal Research 1 (1984) 15–25.

[10] D. Stirling, The sulfur problem: cleaning up industrial feedstock, The Royal Society of Chemistry, 2000.

[11] A.B.M. Heesink, W.P.M. Van Swaaij, The adsorption of H_2S on sulphided limestone, Chem. Eng. Sci. 50 (1995) 3651–3656.

[12] M. Yumura, E. Furlmsky, Comparison of CaO, ZnO, and Fe_2O_3 as H_2S adsorbents at high temperatures, Ind. Eng. Chem. Process Des. Dev. 24 (1985) 1165–1168.

[13] J.M. Davidson, C.H. Lawrie, K. Sohail, Kinetics of the absorption of hydrogen sulfide by high purity and doped high surface area zinc oxide, Ind. Eng. Chem. Res. 34 (1995) 2981–2989.

[14] T. Baird, P.J. Denny, R. Hoyle, F. McMonagle, D. Stirling, J. Tweedy, Modified zinc oxide absorbents for low-temperature gas desulfurisation, J. Chem. Soc., Faraday Trans. 88 (1992) 3375–3382.

[15] N.N. Nassar, M.M. Husein, Study and modeling of iron oxide nanoparticle uptake in AOT (w/o) microemulsions, Langmuir 23 (2007) 13,093–13,103.

[16] O. Lahav, G. Ritvo, I. Slijper, G. Hearne, M. Cochva, The potential of using iron-oxide-rich soils for minimizing the detrimental effects of H_2S in freshwater aquaculture systems, Aquaculture 238 (2004) 263–281.

[17] A.J. Pyzik, S.E. Sommer, Sedimentary iron monosulfides: Kinetics and mechanism of formation, Geochim. Cosmochim. Acta 45 (1981) 687–698.

[18] S.W. Poulton, M.D. Krom, R. Raiswell, A revised scheme for the reactivity of iron (oxyhydr)oxide minerals towards dissolved sulphide, Geochim. Cosmochim. Acta 68 (2004) 3703–3715.

[19] A. Davydov, K.T. Chuang, A.R. Sanger, Mechanism of H_2S oxidation by ferric oxide and hydroxide surfaces, J. Phys. Chem. 102 (1998) 4745–4752.

[20] D.E. Canfield, Reactive iron in marine sediments, Geochim. Cosmochim. Acta 53 (1989) 619–632.

[21] P.R. Westmoreland, D.P. Harrison, Evaluation of candidate solids for high temperature desulfurization of low-btu gases, Environ. Sci. Technol. 10 (1976) 659–661.

[22] R.M. Cornell and U. Schwertmann, The Iron Oxides: Structure, Properties, Occurrences, and Uses; Wiley-VCH, New York, 2nd edition, 2003.

[23] T. Sugimoto, A. Muramatsu, Formation mechanism of monodispersed-Fe_2O_3 particles in dilute $FeCl_3$ solutions, J. Colloid Interface Sci. 184 (1996) 626–638.